Research Article

Nano Research
2023, 16(5): 7364–7372

ISSN 1998-0124 CN 11-5974/O4
https://doi.org/10.1007/s12274-023-5416-5

Cerium oxide nanozymes alleviate oxidative stress in tenocytes for Achilles tendinopathy healing

Xingquan Xu[1,§], Rongliang Wang[1,§], Yixuan Li[1,§], Rui Wu[1], Wenjin Yan[1], Sheng Zhao[2], Quanyi Liu[3,4], Yan Du[3,4], Wenli Gong[1], Weitong Li[1], Hui Wei[2,5] (✉), and Dongquan Shi[1] (✉)

[1] *State Key Laboratory of Pharmaceutical Biotechnology, Division of Sports Medicine and Adult Reconstructive Surgery, Department of Orthopedic Surgery, Nanjing Drum Tower Hospital, The Affiliated Hospital of Nanjing University Medical School, Nanjing 210008, China*

[2] *Department of Biomedical Engineering, College of Engineering and Applied Sciences, Nanjing National Laboratory of Microstructures, Jiangsu Key Laboratory of Artificial Functional Materials, Nanjing University, Nanjing 210023, China*

[3] *State Key Laboratory of Electroanalytical Chemistry, Changchun Institute of Applied Chemistry, Chinese Academy of Sciences, Changchun 130022, China*

[4] *University of Science and Technology of China, Hefei 230026, China*

[5] *State Key Laboratory of Analytical Chemistry for Life Science, School of Chemistry and Chemical Engineering, Chemistry and Biomedicine Innovation Center (ChemBIC), Nanjing University, Nanjing 210023, China*

[§] *Xingquan Xu, Rongliang Wang, and Yixuan Li contributed equally to this work.*

Received: 19 August 2022 / **Revised:** 16 December 2022 / **Accepted:** 17 December 2022

ABSTRACT

Background: Reactive oxygen species (ROS) is considered as ubiquitous and highly active chemicals that influence tendon integrity and orchestrate tendon repair. With significant recent advances in nanomaterials, cerium oxide nanoparticles (CeO_2 NPs) exhibit superoxide dismutase- and catalase-like activities. Herein, we introduced a therapeutic approach of CeO_2 NPs for Achilles tendinopathy (AT) healing. **Methods:** CeO_2 NPs were synthesized to examine their effect as ROS scavengers on AT healing *in vitro* and *in vivo*. The mRNA levels of inflammatory factors were evaluated in AT after CeO_2 NPs treatment *in vitro*. The mechanisms underlying CeO_2 NPs-mediated stimulation of NRF2 translocation and ERK signaling were verified through immunofluorescence and Western blot analysis. The efficacy of CeO_2 NPs was tested in an AT rat model in comparison with the control. **Results:** CeO_2 NPs not only significantly scavenged multiple ROS and suppressed ROS-induced inflammatory reactions but also protected cell proliferation under oxidative stress induced by tert-butyl hydroperoxide (TBHP). Moreover, CeO_2 NPs could promote NRF2 nuclear translocation for anti-oxidation and anti-inflammation through the ERK signaling pathway. In a rat model of collagenase-induced tendon injuries, CeO_2 NPs showed significant therapeutic efficacy by ameliorating tendon damage. **Conclusion:** The present study provides valuable insights into the molecular mechanism of CeO_2 NPs to ameliorate ROS in tenocytes via the ERK/NRF2 signaling pathway, which underscores the potential of CeO_2 NPs for application in the treatment of enthesopathy healing.

KEYWORDS

CeO_2 nanozymes, enthesiopathy, NRF2 translocation, ERK signaling

1 Introduction

Achilles tendinopathy (AT) is a frequent problem in sports medicine, leading to pain and loss of function [1]. Tendinopathic lesions affect both collagen matrix and tenocytes, including disordered collagen fibers, disrupted extracellular matrix homeostasis, and increased inflammatory reactions [2]. Clinical managements have been developed to treat tendinopathy, such as various loading exercises, therapeutic modalities, and surgical interventions [3]. However, some patients still failed to achieve complete relief of tendon symptoms and get back to sports activities, which indicated that a better molecular understanding of tendon healing is required for developing effective treatment strategies.

Healing of ruptured tendons relies on the intrinsic ability of tenocytes to respond to the surrounding stimuli, such as oxidative injury and inflammatory cytokines [4, 5]. Reactive oxygen species (ROS) have been implicated in stress-induced apoptotic pathways, which probably have a role in tendinopathy development [6]. In response to tissue injury, tenocytes also release pro-inflammatory cytokines such as IL-1β and IL-6 to regulate tendon extracellular matrix remodeling [7]. Though live organisms have evolved a number of natural enzymes to scavenge ROS and protect tissues from inflammation-induced damages [8], they are neither stable nor immunologically tolerant, and hard to mass-produce [9]. Therefore, intensive efforts have been made to develop ROS scavenging artificial enzymes to overcome the inherent drawbacks of natural enzymes.

An increasing number of studies have showed that cerium oxide nanoparticles (CeO_2 NPs), one of catalytic nanomaterials

Address correspondence to Hui Wei, weihui@nju.edu.cn; Dongquan Shi, shidongquan@nju.edu.cn

with natural enzyme-like activities (i.e., nanozymes), exhibit ROS scavenging activities in many ROS-related diseases. CeO_2 NPs have the ability to mimic superoxide dismutase (SOD)- and catalase (CAT)-like activity due to the mixed valance states of Ce^{3+} and Ce^{4+} [10]. This catalytic anti-oxidant activity makes CeO_2 NPs a therapeutics to reduce inflammation through ROS scavenging for treating inflammatory bowel disease (IBD) [11]. Furthermore, CeO_2 NPs scavenged multiple ROS and suppressed ROS-induced inflammatory reactions in periodontitis [12]. Hence, we hypothesized that CeO_2 NPs could greatly decrease the excessive ROS and thus be a promising therapeutic for periodontitis treatment.

Herein, we synthesized CeO_2 NPs and investigated their use as an antioxidant and anti-inflammatory agent for AT management. *In vitro*, CeO_2 NPs significantly reduced ROS and inflammation induced by an exogenous agent, tert-butyl hydroperoxide (TBHP) via the ERK/NRF2 signaling pathway in tenocytes. *In vivo*, CeO_2 NPs were employed to repair the injured tendons in collagenase-induced AT rats, which indicated the promising therapeutic effect of nanozymes in the treatment of enthesopathy healing.

2 Materials and methods

2.1 Materials and reagents

Cerium nitrate hexahydrate ($Ce(NO_3)_3{\cdot}6H_2O$, 99.95%), ethylene glycol (98%), and ammonia solution (NH_4OH, 25%–28%) were purchased from Aladdin (Shanghai, China). Tert-butyl hydroperoxide solution was bought from Sigma-Aldrich (Darmstadt, Germany). PD98059 was purchased from MedChem Express (Monmouth Junction, NJ, USA). The primary antibodies against NRF2 were offered by Proteintech (IL, USA). The goat anti-rabbit HRP-labeled secondary antibody was obtained from Fude Biological Technology (Hangzhou, China). The antibodies against p-ERK, ERK, histone H3, and GAPDH were provided by Cell Signaling Technology (Danvers, MA, USA). Collagenase type I was obtained from GIBCO BRL (Grand Island, NY, USA). Votalin emulgel was bought from Glaxo Smith Kline (Brentford, Middlesex, UK).

2.2 Synthesis and characterization of CeO_2

CeO_2 NPs were prepared as described previously [13]. Briefly, 504 mg $Ce(NO_3)_3{\cdot}6H_2O$ was added to 20 mL of water-ethylene glycol solution, and vigorously stirred at 60 °C for 10 min. Then, 3.2 mL of NH_4OH was rapidly added into the mixture with vigorous stirring for 3 h. After centrifugation, the CeO_2 NPs were washed with deionized water, followed by modification with citric acid, and pH adjustment to 7.0 with sodium citrate. Finally, the purified products were dispersed into deionized water as a highly transparent solution for further use. The transmission electron microscope (TEM) results of CeO_2 morphology, structure, and size were measured on an FEI TECNAI F20 at an acceleration voltage of 200 kV. The Cu Kα radiation was used to collect X-ray diffraction (XRD) data on a Rigaku Ultima diffractometer with 2°/min.

2.3 SOD-mimicking activity of CeO_2

According to the protocol of a SOD assay kit (Dojindo), 20 μL of CeO_2 solution with different concentrations was added with 200 μL of WST-1 solution in a microplate well. Subsequently, the mixture was added with 20 μL of enzyme working solution, thoroughly mixed, and placed at 37 °C for 20 min. Finally, the absorbance data were measured on a microplate reader at 450 nm [14].

2.4 CAT-mimicking activity of CeO_2

According to the protocol of a CAT assay kit, 5 μL of CeO_2 solution with different concentrations was added with 90 μL of buffer solution in a microplate well. Subsequently, 100 μL of working solution and 5 μL of H_2O_2 were rapidly added in each well. Then, the microplate transferred into an anaerobic pouch at 37 °C for 30 min, and the absorbance was detected at 405 nm [13].

2.5 Animal study

Adult male Sprague–Dawley (SD) rats (250–300 g, n = 40) were purchased from the Animal Center of Nanjing Medical University (Jiangsu, China). Rats were acclimated in regular cages at 24 °C under a 12-h light/dark cycle for 1 week. Animal experiments were performed in accordance with the guidelines of the Ethics Committee of Drum Tower Hospital, Medical School of Nanjing University, Nanjing, China (Ethics approval No. 20200413).

After acclimation, thirty rats were used in the establishment of AT, and the other ten rats were experienced sham operation. As described, 50 μL of collagenase I solution (5 mg/mL) was injected in the rat right hind leg every 2 days to mimic the Achilles tendon injury model. After 14 days to establish the AT models, the rats were randomly divided into three groups: the Control (Ctrl) group, Votalin group, and CeO_2 group. For the following experiments, 25 μg/mL CeO_2 was injected into the same side of injured tendon twice a week, and the Ctrl group was treated with same volume of physiological saline. The rats in the Votalin group received 1 mg Votalin treatment per rat. After 14 days, all the tendons and major organs from these four groups were harvested and prepared for further histological analysis.

2.6 Histopathologic analysis

Tendon samples were immediately immersed in 4% paraformaldehyde solution after sacrificed the rats. These tissues were experienced with a graded dehydration of ethanol series and finally embedded in paraffin, which were sliced into pieces of 5 μm then. After dewaxed and stained with hematoxylin-eosin (HE) and Masson's trichrome, the slices were observed under a fluorescence microscope (Zeiss Inc., Heidelberg, Germany).

2.7 Immunohistochemistry analysis

After dewaxed and rehydration, tissue sections were quenched endogenous peroxidase activity with 3% hydrogen peroxide. Then, the sections were experienced antigen retrieval with 0.4% pepsin (Sigma-Aldrich) treatment at 37 °C for 1 h. Before incubated with primary antibody overnight at 4 °C, the sections were blocked with 10% goat serum for 30 min at 37 °C. After incubation with an horse radish peroxidase (HRP)-conjugated secondary antibody, immunohistochemical staining was using an ultra-sensitive DAB Kit and photographed by a fluorescence microscope (Zeiss Inc., Heidelberg, Germany).

2.8 Isolation and culture of tendinocytes

The harvested rat tendons were wasted and rinsed with cold sterile phosphate buffered saline (PBS). After being minced into 1 mm^3 pieces, the tendon tissues were digested with 3 mg/mL collagenase I solution overnight at 37 °C. After filtration and centrifugation, the pellet was placed in Dulbecco's modified Eagle medium (DMEM)/F12 medium with 10% fetal bovine serum. The primary cells were cultured in 5% CO_2 at 37 °C and the medium was replaced every 2 or 3 days thereafter. The third or fourth generation long fusiform cells were used for *in vitro* experiments.

2.9 Cell viability assay

Tenocytes (1×10^4 cells/well) were seeded in a 96-well plate and

then treated with different concentrations of CeO_2 for 24 h. After incubated with TBHP for 12 h, the cell viability was evaluated with the cell counting kit-8 (CCK-8) assay (Dojindo Co, Kumamoto, Japan) according to the manufacturer's protocol. The experiment was performed in triplicate and the data were averaged.

2.10 ROS levels measurement

ROS levels were determined by using a fluorescence microscope or flow cytometry. For fluorescence imaging, tenocytes (2×10^5 cells/well) were plated in 6-well plates and then treated with TBHP with or without different concentrations of CeO_2. Then, the cells were stained with 2′ ,7′ -dichlorodihydrofluorescein diacetate (DCFH-DA) (Beyotime, Shanghai, China) at 37 °C for 30 min. ROS levels were directly visualized under a fluorescence microscope (Zeiss Inc., Heidelberg, Germany). Or the cells were washed three times after incubation with DCFH-DA, and diluted in flow buffer. The ROS levels were evaluated through a BD AccuriC6 Plus Flow CytoMeter (BD Biosciences, USA) based on the absorption values divided by control group.

2.11 Quantitative real-time PCR (qRT-PCR) analysis

The RNA-quick Purification Kit (ES Science, Shanghai, China) was used to extract the total RNA from tenocytes according to the manufacturer's instructions. After measuring RNA concentrations, same amount of RNA was reverse-transcribed into cDNA. Synthesized cDNAs were conducted for qRT-PCR using SYBR Color quantitative polymerase chain reaction (qPCR) Master Mix (Vazyme Biotech, Nanjing, China). The primer sequences of mRNAs are shown in Table S1 in the Electronic Supplementary Material (ESM).

2.12 Western blot analysis

After the different treatments, tenocytes were washed twice. Then, radioimmunoprecipitation assay (RIPA) lysis buffer was used to extract total protein. And a nuclear and cytosolic extraction reagent Kit (Solarbio, Beijing, China) was used to purify cytosolic and nuclear proteins. After centrifuging, the protein concentrations were determined using a BCA protein assay reagent kit (Thermo Scientific, MA, USA). The equal amount of protein samples was separated on a 10% polyacrylamide gel and then transferred onto polyvinylidene fluoride membranes (Bio-Rad, Hercules, CA, USA). After being blocked with 5% milk for 1 h at room temperature, the membranes were cut into sections and incubated with the following primary antibodies: NRF2, p-ERK, and ERK at 4 °C overnight. Next, the membranes were incubated with the appropriate HRP-conjugated secondary antibodies for 1 h. The protein and band signals were detected using a ChemiDocXRS Imaging System (Tanon, Shanghai, China).

2.13 Immunofluorescence analysis

Tenocytes (5×10^4 cells/well) were fixed in 4% paraformaldehyde for 15 min, and permeabilized with 0.1% Triton X-100 for 15 min. After blocked with 5% bovine serum albumin (BSA) for 1 h at room temperature, the slides were incubated with primary antibodies at 4 °C overnight. Followed by staining with fluorescein isothiocyanate (FITC)-conjugated anti-rabbit antibody for 60 min at room temperature in the dark, the slides were counterstained with 4',6-diamidino-2–phenylindole (DAPI) for 5 min. The images were captured by fluorescence microscopy (Zeiss Inc., Heidelberg, Germany). The distribution of NRF2 around the nuclear zone was quantified along 80 μm wide lines. The fluorescence line intensity plots were performed using ImageJ as described before [14].

2.14 Short interfering RNA (siRNA) transfection

A siRNA against the rat NRF2 gene was designed and synthesized by Hippobio (Huzhou, China): si-NRF2 (s) 5'-GCAGG ACAUGGAUUUGAUU-3', (as) 5'-AAUCAAAUCCAUGUCC UGC-3'. The tenocytes were cultured in 60 mm Petri dishes at a density of 2×10^5/mL and cultured to 60%–70% confluency. Then, transfection of si-NRF2 or negative control (Scr) and transfected was achieved using Lipofectamine 3000 siRNA reagent (Invitrogen, Carlsbad, CA, USA). The silencing efficiency was determined by qPCR and Western blot analysis.

2.15 Statistical analysis

All the assays were performed in triplicate. The quantitative data were presented as the mean ± standard deviation (SD). The statistical significance among the groups was determined by one-way analysis of variance (ANOVA) followed by Tukey post hoc analysis using GraphPad Prism 7. Results were considered as a significant difference when P value < 0.05 compared with other groups.

3 Results

3.1 Characterization and ROS scavenging activities of CeO_2

We used a wet-chemical method to prepare the CeO_2 nanozymes [11]. As shown in Figs. 1(a) and 1(b), well-dispersed CeO_2 NPs with clear lattice fringes were observed by TEM. The CeO_2 NPs had an average diameter of 4.12 ± 0.85 nm (Fig. 1(b)). The XRD spectra exhibited the characteristic peaks of CeO_2 at 2θ of 28.5°, 32.9°, 47.4°, and 56.8°, showing the high crystallinity of the prepared CeO_2 (Fig. 1(d)). Due to the redox cycle of Ce^{4+}/Ce^{3+} and oxygen vacancies, CeO_2 has the property to scavenge ROS. The SOD-mimicking activity of CeO_2 was investigated by using a WST-1 assay kit. The $-O_2\cdot$ elimination efficiency of 1.0, 2.5, 10.0, and 20.0 μg/mL CeO_2 was 29.8% ± 10.5%, 41.7% ± 5.3%, 66.8% ± 3.0%, and 87.2% ± 0.1%, respectively. The catalytic activity was positively correlated with the concentration of CeO_2 (Fig. 1(e)). Then, the CAT mimicking activity of CeO_2 was investigated by detecting the released oxygen during the decomposition of H_2O_2 with a CAT assay kit, which was measured at 405 nm. Similarly, the oxygen generation was largely reduced by CeO_2 in a concentration-dependent manner (Fig. 1(f)). Thus, the above results demonstrate the advantage of CeO_2 as an ROS scavenger, indicating the antioxidant protective potential towards cells.

3.2 CeO_2 reduced TBHP-induced oxidative stress and inflammatory response

Then, we evaluated the antioxidant protective activity of CeO_2 at the cellular level. It should be noted that CeO_2 NPs were non-toxic to tenocytes, even showing a significantly good biocompatibility for a long-time co-culture (Fig. 2(a)). Upon the oxidative stimulation of TBHP (30 μmol/L), the viability of tenocytes was significantly decreased by more than 30% according to the CCK-8 assay (Fig. 2(b)). However, the cells could be rescued by CeO_2 NPs (25 and 50 μg/mL) (Fig. 2(c)). Moreover, the mRNA levels of inflammatory factors, including IL-1β and IL-6, were detected by qRT-PCR. Compared to the Ctrl group, TBHP-induced oxidative stress increased the expression of IL-1β and IL-6 in tenocytes. Interestingly, this inflammatory response was alleviated by CeO_2 NPs treatment (Fig. 2(d)). In addition, the results of these inflammation cytokines release were highly consistent with the

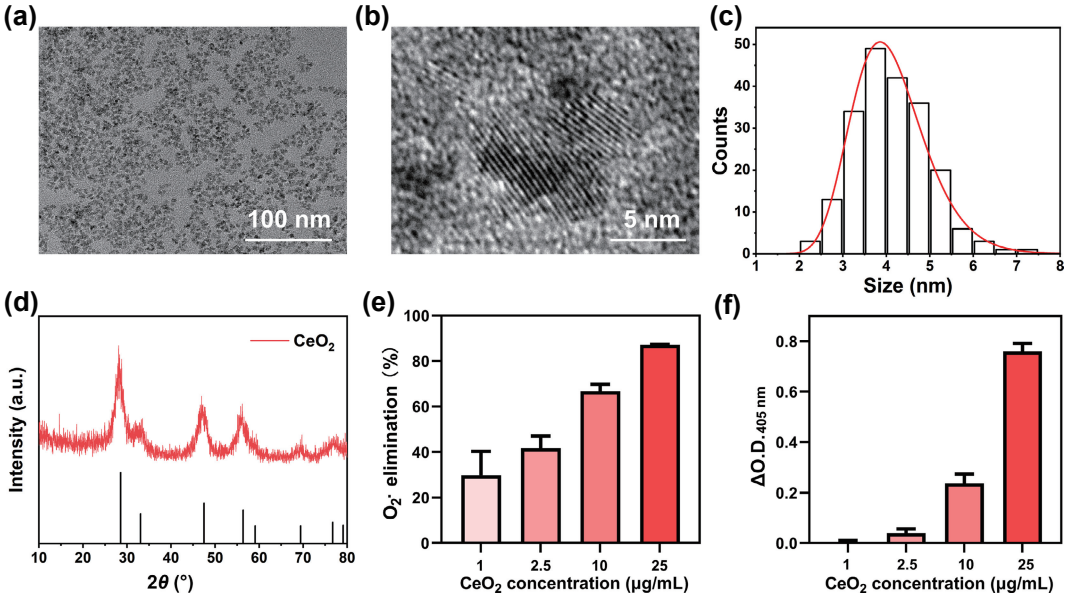

Figure 1 Characterization and ROS scavenging activities of CeO_2. (a) TEM and (b) high-resolution TEM images of CeO_2. (c) Size distribution of CeO_2 (n = 3). (d) XRD pattern of CeO_2. (e) SOD-mimicking activity and (f) CAT-mimicking activity.

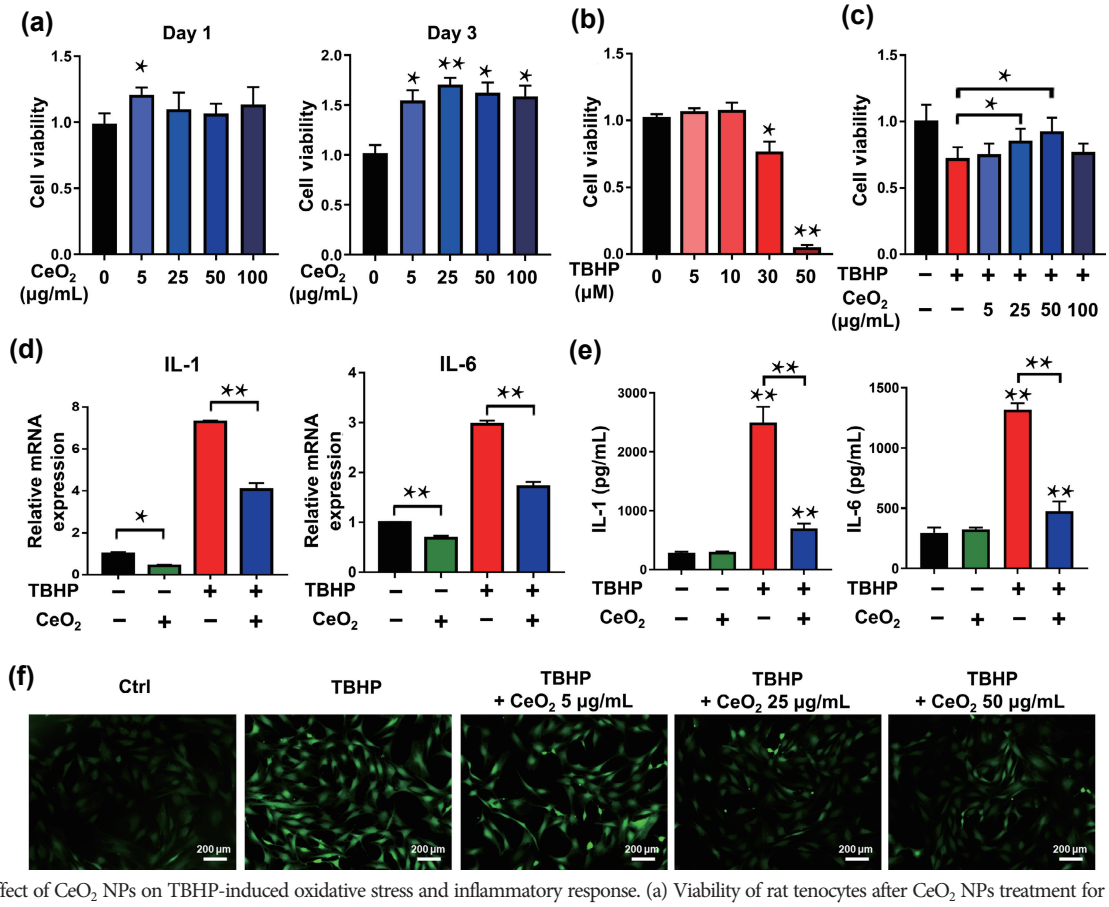

Figure 2 Effect of CeO_2 NPs on TBHP-induced oxidative stress and inflammatory response. (a) Viability of rat tenocytes after CeO_2 NPs treatment for 1 and 3 days. (b) Viability of rat tenocytes after TBHP treatment. (c) Viability of rat tenocytes after TBHP treatment with or without CeO_2 NPs. (d) and (e) qPCR and ELISA analysis of IL-1 and IL-6 levels in tenocytes stimulated with TBHP and treated with or without CeO_2 NPs. (f) Fluorescence images of the ROS generated after cells were co-incubated with or without CeO_2 NPs after TBHP stimulation (green fluorescence refers to ROS). * $p < 0.05$, ** $p < 0.01$.

above observation (Fig. 2(e)). Moreover, CeO_2 NPs treatment also decreased the changes in cellular ROS following TBHP challenge. Fluorescence analysis showed a markedly decreased density of TBHP-induced ROS in tenocytes after CeO_2 NPs treatment in a dose-dependent manner (Fig. 2(f) and Fig. S1(a) in the ESM). These findings support the hypothesis that CeO_2 NPs could act as an ROS scavenger to attenuate oxidative stress and inflammation to protect tenocytes.

3.3 CeO_2 increased NRF2 expression for anti-oxidation and anti-inflammation

Instances of sustained oxidative activity have been shown to influence NRF2 signaling [15]. Therefore, the effect of CeO_2 on NRF2 expression was studied. First, we confirmed the increased NRF2 expression in oxidatively stressed tenocytes by using TBHP. Western blot analysis revealed that TBHP led to a light activation of NRF2 signaling, not significant, in response to oxidative stress,

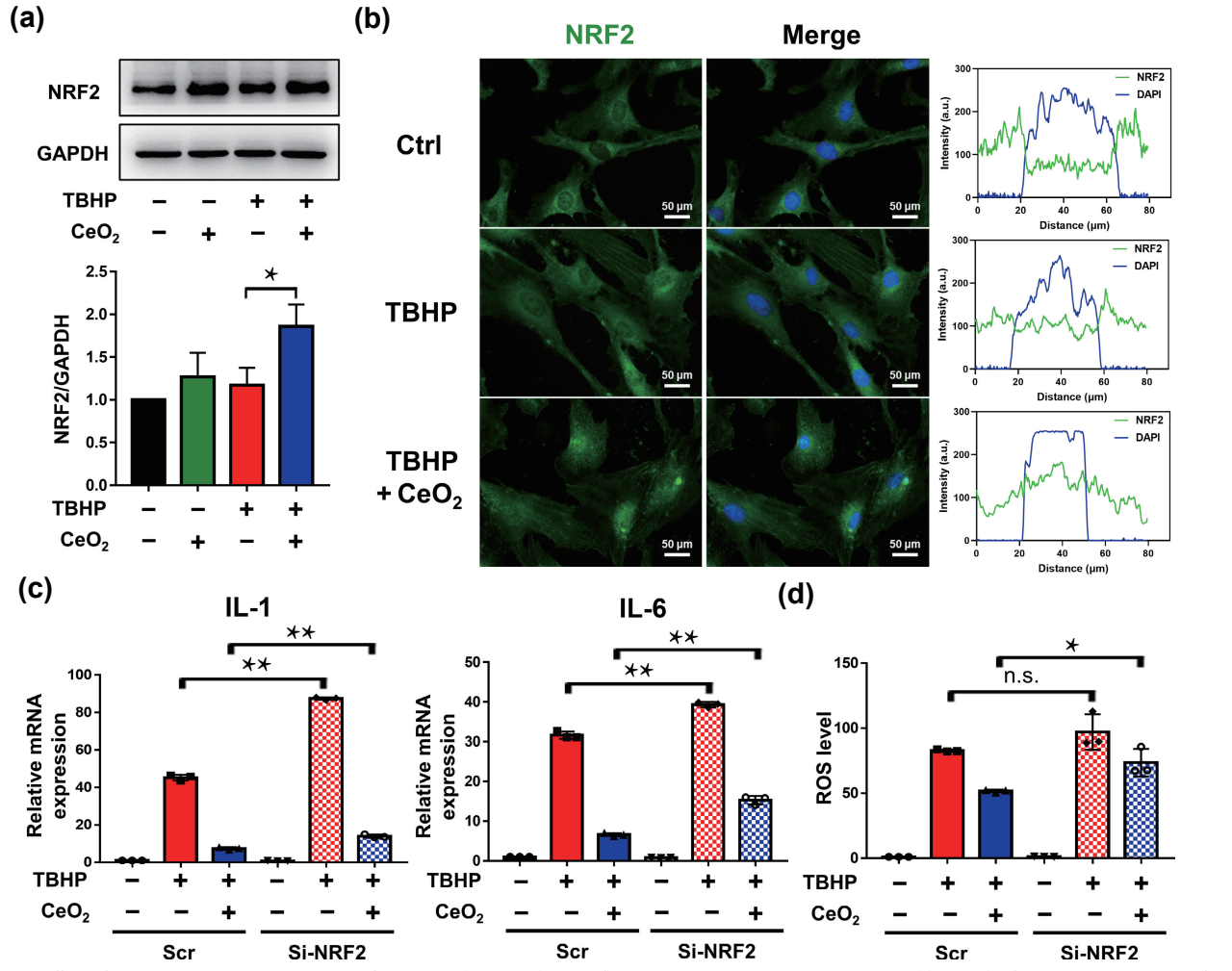

Figure 3 Effect of CeO_2 NPs on NRF2 expression for anti-oxidation and anti-inflammation. (a) Representative Western blot results for NRF2 in tenocytes after TBHP stimulation with or without CeO_2 NPs treatment. (b) Immunofluorescence image and the fluorescence line intensity plots of NRF2 in tenocytes stimulated with TBHP and treated with or without CeO_2 NPs. (c) The mRNA levels of IL-1 and IL-6 in tenocytes stimulated with TBHP alone, or treated with CeO_2 NPs combined with scrambled siRNAs (Scr) or Si-NRF2. (d) Flow cytometry analysis of the ROS in tenocytes stimulated with TBHP alone, or treated with CeO_2 NPs combined with Scr or Si-NRF2. * $p < 0.05$, ** $p < 0.01$, n.s., not significant.

and the NRF2 expression was further enhanced by CeO_2 NPs treatment (Fig. 3(a)). Furthermore, immunofluence analysis confirmed that CeO_2 NPs increased NRF2 levels in nuclear fractions rather than cytosolic fractions after exposing to TBHP (Fig. 3(b)). To directly corroborate the involvement of NRF2 in anti-oxidation and anti-inflammation of CeO_2 NPs, stealth siRNA was employed to specifically inhibit the expression of NRF2 protein in tenocytes (Figs. S1(b) and S1(c) in the ESM). Meanwhile, the levels of inflammatory cytokines (IL-1 and IL-6) and ROS increased when si-NRF2 was used (Figs. 3(c) and 3(d)), reflecting the anti-inflammatory and anti-oxidative activities of CeO_2 NPs were suppressed.

3.4 CeO_2-mediated ERK signaling activation promoted NRF2 nuclear translocation for anti-oxidation and anti-inflammation

We further found that p-ERK expression was slightly decreased after TBHP stimulation in tenocytes. The decrease was reversed by CeO_2 NPs treatment in a dose-dependent manner (Fig. 4(a)). Of note, the NRF2 expression was significantly increased in nuclear localization rather than cytosolic localization following stimulation with TBHP, which was further enhanced by CeO_2 NPs treatment. Moreover, the nuclear NRF2 expression was significantly decreased when an ERK signaling inhibitor (PD98058) was added (Fig. 4(b)). Consistent with Western blot analysis, immunofluorescent images showed that CeO_2 NPs promoted NRF2 nuclear translocation, and the density of NRF2 in the nucleus was decreased after ERK signaling inhibition in tenocytes (Fig. 4(c)). Notably, significant enhancements in the levels of IL-1β, IL-6, and intracellular ROS were observed after NRF2 expression was decreased by PD98059 treatment (Figs. 4(d) and 4(e)). These observations indicate that the ERK/NRF2 signaling pathway plays an important role in anti-inflammation and anti-oxidation for CeO_2 NPs in tenocytes.

3.5 CeO_2 NPs increased NRF2 expression and ameliorated impairment of tendon fibers in AT rats

After investigating the ROS scavenging activity and anti-inflammatory effect of CeO_2 NPs in cells, we studied their protective efficacy in AT rats. Compared to the Ctrl group, AT tissue sections in the Votalin group showed a much more regular and compact alignment of collagen fibers according to the results of HE staining. At the same time, the disorganized and incompact collagen fibers in the tendinopathy group could also be arranged orderly and tightly after the treatment with CeO_2 NPs. As depicted in Masson trichrome staining, severe disruption of collagen fibril organization was observed in the Ctrl group. However, the Votalin treatment and CeO_2 treatment prevented collagen matrix disruption and disorganization. Moreover, Col1 expression was significantly upregulated following the application of votalin treatment and CeO_2 NPs treatment (Fig. 5(a)). In addition,

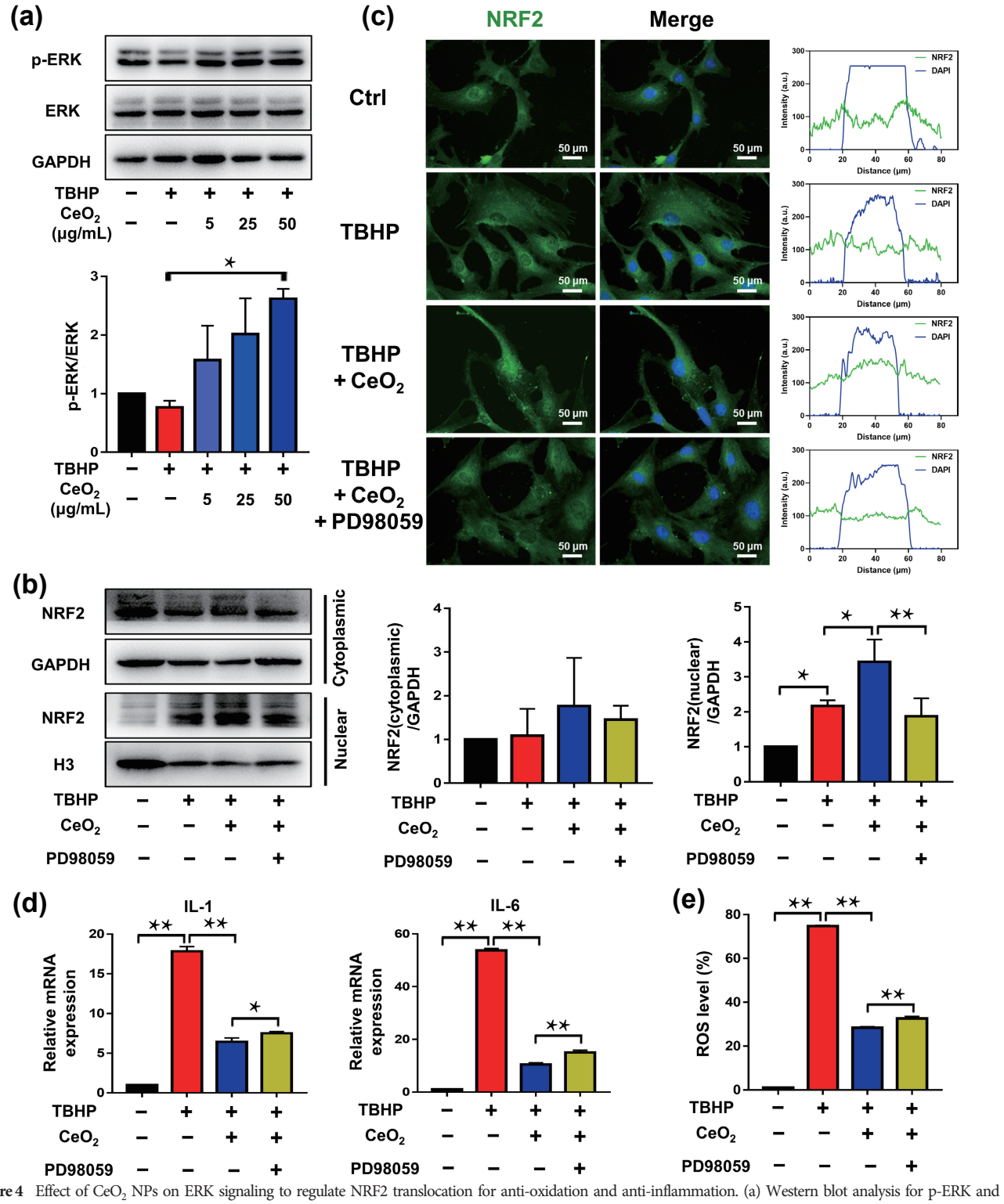

Figure 4 Effect of CeO_2 NPs on ERK signaling to regulate NRF2 translocation for anti-oxidation and anti-inflammation. (a) Western blot analysis for p-ERK and ERK in tenocytes after TBHP stimulation with or without CeO_2 NPs treatment. (b) Western blot analysis for nuclear and cytoplasmic expression of NRF2 in tenocytes treated with TBHP and TBHP + CeO_2 NPs with or without PD98059. (c) Immunofluorescence images and the fluorescence line intensity plots of NRF2 in tenocytes treated with TBHP and TBHP + CeO_2 NPs with or without PD98059. (d) The mRNA levels of IL-1 and IL-6 in tenocytes treated with TBHP and TBHP + CeO_2 NPs with or without PD98059. (e) Flow cytometry analysis of the ROS in tenocytes treated with TBHP and TBHP + CeO_2 NPs with or without PD98059. * $p < 0.05$, ** $p < 0.01$.

although a higher NRF2 expression was observed in AT tissue sections of the Ctrl and Votalin groups, NRF2 was more enriched in the nuclei of tenocytes treated with CeO_2 NPs (Fig. 5(b)).

4 Discussions

In this study, we introduced CeO_2 NPs as an ROS scavenger to ameliorate oxidative stress and inflammatory reactions in tenocytes via stimulation of the ERK/NRF2 signaling pathway. In the AT rat model, our therapeutic strategy to use CeO_2 NPs for promotion of tendon healing process lays a solid foundation for future clinical application of nanozymes in the treatment of enthesopathy healing.

Scavenging ROS and amelioration of oxidative stress as important strategies influence the propensity for tendinopathic development and repair. Tendinopathies have a complex pathological process. Currently, different theories are proposed to

illustrate the pathways contributing to the etiology of tendinopathies, such as mechanical theory, inflammation theory, and apoptosis theory [16]. Therefore, multiple therapies have been advocated in patients with tendinopathy, including physiotherapy, nonsteroidal anti-inflammatory drugs (NSAIDs), and local injections of glucocorticoids [17]. ROS, a universal factor to impose cellular/tissue damage, is reported to be associated with oxidative damage in chronic tendinopathy, suggesting the participation of ROS in tendon degeneration, failure, or healing [18–20]. A previous study reported that effective attenuation of oxidative stress could ameliorate the activation of endoplasmic reticulum (ER) stress, which indicated a strategy to prevent and treat AT [21]. In addition, excessive ROS release was found to be associated with the NF-κB signaling pathway. Therefore, the complex interaction may participant in the modulation of inflammation and apoptosis and recover the collagen component of the extracellular matrix in tendinopathy [22, 23]. Inflammatory response was reported to be triggered in the tendon tissue with the release of inflammatory cytokines, such as iNOS, COX-2, TNF-α, and IL-1β [24, 25]. In accordance with this information, this study showed that treatment of CeO_2 NPs, an effective ROS scavenger, prevented TBHP-induced overproduction of ROS and cell death in tenocytes. Additionally, CeO_2 NPs had an anti-inflammatory effect to decrease the expressions of IL-1β and IL-6 proinflammatory cytokines induced by TBHP. Therefore, it was thought that CeO_2 NPs exhibited a better AT healing than Votalin (a nonsteroidal anti-inflammatory drug) because of their antioxidant properties and thus exerted an anti-inflammatory effect.

Nanozymes possess great promise in the clinical management of enthesopathy healing. Because of their enzyme mimicking acitivity and multifunctionality, nanozymes are advantageous over natural enzymes, such as low-cost, high stability, and mass-production [26]. CeO_2 NPs are among the first reported nanomaterials with SOD-mimicking activities and have been reported to exhibit CAT-like activities to eliminate NO and ·OH as well [27]. Therefore, CeO_2 NPs have been regarded as a creditable ROS scavenger for neuroprotection, which was characterized as ROS generated and accumulated during the ischemic process [28, 29]. As a result, several studies also reported biocompatible nanoceria with anti-inflammation effects [30], such as acute hind paw inflammation [31], liver damage [32], and

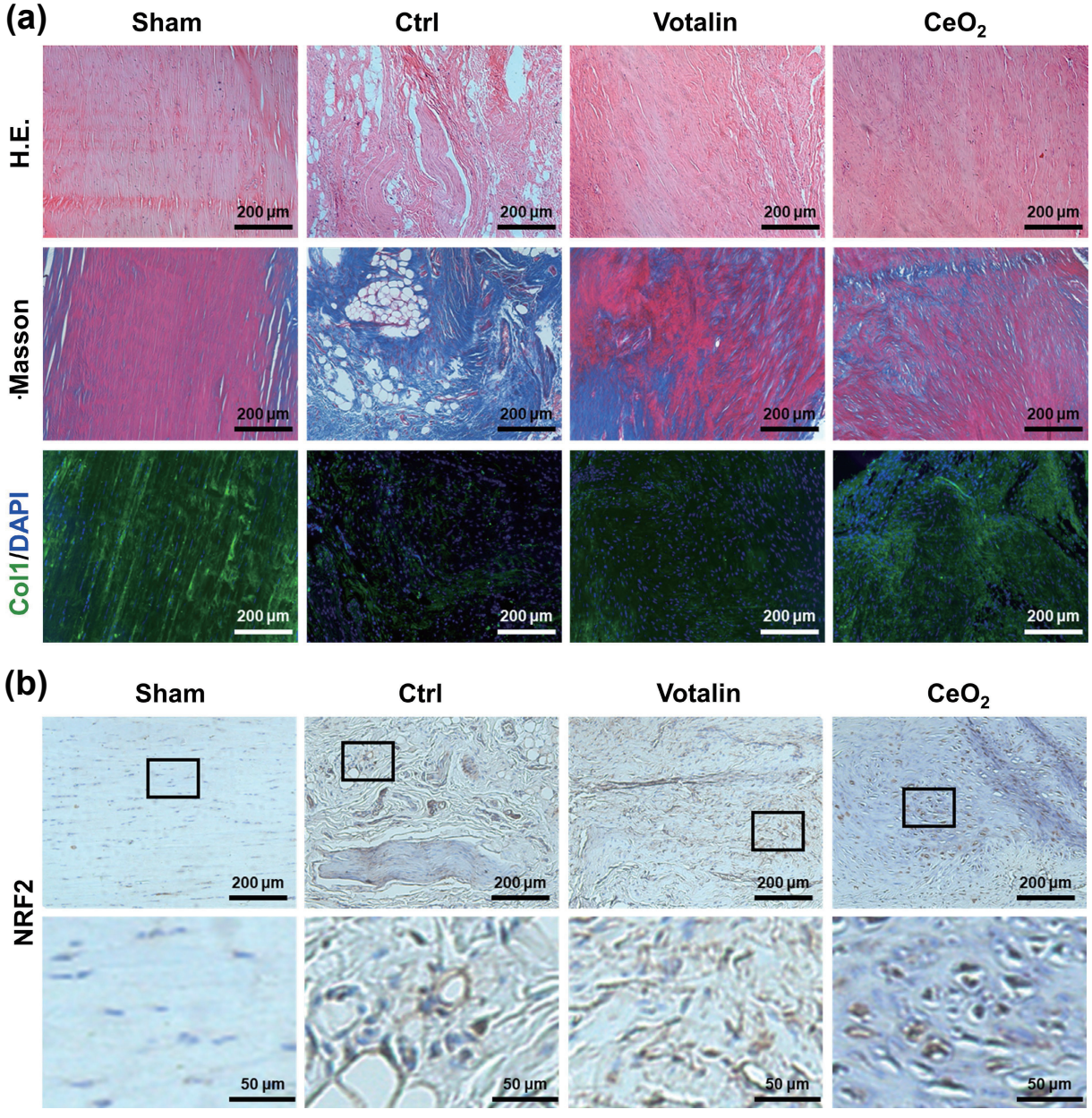

Figure 5 Effect of CeO_2 NPs on NRF2 expression in Achilles tendinopathy rats. (a) HE staining, Masson staining, and immunofluorescence analysis of Collagen 1 in the four groups (Sham, Ctrl, Votalin, and CeO_2). (b) Immunohistochemical staining for NRF2 in the injured tendon of rats with/without indicated treatment.

sepsis [33]. Based on prior work, we propose a new application of CeO_2 in AT healing. Particularly, benefiting from the antioxidant and anti-inflammatory properties of CeO_2, a better treatment effect on proliferation-promoting and inhibiting matrix degradation in tendon injury sites could be obtained compared with current options. Besides, nanozymes like CeO_2 NPs could be promising candidates for enthesopathy and related biomedical fields.

CeO_2 NPs attenuate enthesis repair by modulating the ERK/NRF2 pathway. NRF2 exerts protective role on cell and tissue damage caused by oxidative stress by balancing the oxidation and anti-oxidation activities [34]. Previous studies have proposed that NRF2 is of major importance for the positive effect on tendon cell growth and tendon regeneration [35]. Moreover, the MAP kinases ERK can activate the NRF2-mediated antioxidant response, and relative analysis showed that CeO_2 NPs reverted the H_2O_2-mediated increase in the phosphorylation of MAPK/ERK signaling pathways [36, 37]. Our results were consistent with these findings and showed that ERK/NRF2 signaling participant in the improvement of CeO_2 NPs on TBHP-induced oxidative stress and apoptosis effect. The ROS scavenging activity of CeO_2 NPs directly attenuated the high levels of ROS, and ERK signaling activation induced by CeO_2 NPs provided powerful antioxidant support. All above protective effect of CeO_2 NPs potentially improved collagenase-related tendon pathological dysfunctions by activating the NRF2 expression.

The current study can be improved in several aspects. Firstly, we did not evaluate the collagen regeneration of tenocytes under the treatment of CeO_2 NPs. We were not sure whether the ERK/NRF2 signaling activation regulated collagen expression during this process. Third, the local injection method still has the possibility to induce tendons injury in our animal experiments. To overcome these limitations, further research could carry out more detailed mechanism study and explore the application of injectable gel or microneedles loaded with CeO_2 NPs for clinical therapy [38, 39].

5 Conclusions

In brief, we demonstrated that CeO_2 NPs exhibited high SOD- and CAT-like activity and protected tenocytes from oxidative stress through the ERK/NRF2 pathway activation. A rat model of tendinopathy revealed that CeO_2 NPs treatment was a practical approach to improve the quality of tendon healing, which indicated a novel therapeutic strategy for tendon repair in the future.

Acknowledgements

This work was supported by the National Natural Science Foundation of China (Nos. 81941009, 81991514, 32271409, and 82202778), Nanjing Distinguished Youth Fund (No. JQX20001), Jiangsu Provincial Key R&D Program (No. BE2022836), China Postdoctoral Science Foundation (No. 2020M671456), National Basic Research Program of China (No. 2021YFA1201404), Jiangsu Provincial Key Medical Center Foundation, Jiangsu Provincial Medical Outstanding Talent Foundation, Jiangsu Provincial Medical Youth Talent Foundation and Jiangsu Provincial Key Medical Talent Foundation, and the Fundamental Research Funds for the Central Universities (Nos. 14380493 and 14380494).

Electronic Supplementary Material: Supplementary material (quantification of ROS level (Fig. S1(a)), siRNA efficiency (Figs. S1(b) and S1(c)), and primer sequences used for qPCR (Table S1)) is available in the online version of this article at https://doi.org/10.1007/s12274-023-5416-5.

References

[1] De Jonge, S.; Van Den Berg, C.; De Vos, R. J.; Van Der Heide, H. J. L.; Weir, A.; Verhaar, J. A. N.; Bierma-Zeinstra, S. M. A.; Tol, J. L. Incidence of midportion Achilles tendinopathy in the general population. *Br. J. Sports Med.* **2011**, *45*, 1026–1028.

[2] Magnusson, S. P.; Langberg, H.; Kjaer, M. The pathogenesis of tendinopathy: Balancing the response to loading. *Nat. Rev. Rheumatol.* **2010**, *6*, 262–268.

[3] Vo, T. P.; Ho, G. W. K.; Andrea, J. Achilles tendinopathy, a brief review and update of current literature. *Curr. Sports Med. Rep.* **2021**, *20*, 453–461.

[4] Murrell, G. A. C. Oxygen free radicals and tendon healing. *J. Shoulder Elbow Surg.* **2007**, *16*, S208–S214.

[5] Millar, N. L.; Murrell, G. A. C.; McInnes, I. B. Alarmins in tendinopathy: Unravelling new mechanisms in a common disease. *Rheumatology (Oxford).* **2013**, *52*, 769–779.

[6] Bestwick, C. S.; Maffulli, N. Reactive oxygen species and tendinopathy: Do they matter? *Br. J. Sports Med.* **2004**, *38*, 672–674.

[7] Millar, N. L.; Murrell, G. A. C.; McInnes, I. B. Inflammatory mechanisms in tendinopathy—towards translation. *Nat. Rev. Rheumatol.* **2017**, *13*, 110–122.

[8] Li, X. Y.; Fang, P.; Mai, J.; Choi, E. T.; Wang, H.; Yang, X. F. Targeting mitochondrial reactive oxygen species as novel therapy for inflammatory diseases and cancers. *J. Hematol. Oncol.* **2013**, *6*, 19.

[9] Yao, J.; Cheng, Y.; Zhou, M.; Zhao, S.; Lin, S. C.; Wang, X. Y.; Wu, J. J. X.; Li, S. R.; Wei, H. ROS scavenging Mn_3O_4 nanozymes for *in vivo* anti-inflammation. *Chem. Sci.* **2018**, *9*, 2927–2933.

[10] Korsvik, C.; Patil, S.; Seal, S.; Self, W. T. Superoxide dismutase mimetic properties exhibited by vacancy engineered ceria nanoparticles. *Chem. Commun.* **2007**, 1056–1058.

[11] Zhao, S.; Li, Y. X.; Liu, Q. Y.; Li, S. R.; Cheng, Y.; Cheng, C. Q.; Sun, Z. Y.; Du, Y.; Butch, C. J.; Wei, H. An orally administered CeO_2@montmorillonite nanozyme targets inflammation for inflammatory bowel disease therapy. *Adv. Funct. Mater.* **2020**, *30*, 2004692.

[12] Yu, Y. J.; Zhao, S.; Gu, D. A.; Zhu, B. J.; Liu, H. X.; Wu, W. L.; Wu, J. J. X.; Wei, H.; Miao, L. Y. Cerium oxide nanozyme attenuates periodontal bone destruction by inhibiting the ROS-NF κB pathway. *Nanoscale* **2022**, *14*, 2628–2637.

[13] Lin, A. Q.; Liu, Q. Y.; Zhang, Y. H.; Wang, Q.; Li, S. R.; Zhu, B. J.; Miao, L. Y.; Du, Y.; Zhao, S.; Wei, H. A dopamine-enabled universal assay for catalase and catalase-like nanozymes. *Anal. Chem.* **2022**, *94*, 10636–10642.

[14] Farías, G. G.; Guardia, C. M.; Britt, D. J.; Guo, X. L.; Bonifacino, J. S. Sorting of dendritic and axonal vesicles at the pre-axonal exclusion zone. *Cell Rep.* **2015**, *13*, 1221–1232.

[15] Rizvi, F.; Shukla, S.; Kakkar, P. Essential role of pH domain and leucine-rich repeat protein phosphatase 2 in Nrf2 suppression via modulation of Akt/GSK3β/Fyn kinase axis during oxidative hepatocellular toxicity. *Cell Death Dis.* **2014**, *5*, e1153.

[16] Millar, N. L.; Silbernagel, K. G.; Thorborg, K.; Kirwan, P. D.; Galatz, L. M.; Abrams, G. D.; Murrell, G. A. C.; McInnes, I. B.; Rodeo, S. A. Tendinopathy. *Nat. Rev. Dis. Primers* **2021**, *7*, 1.

[17] Challoumas, D.; Biddle, M.; Millar, N. L. Recent advances in tendinopathy. *Fac. Rev.* **2020**, *9*, 16.

[18] Riley, G. Chronic tendon pathology: Molecular basis and therapeutic implications. *Expert Rev. Mol. Med.* **2005**, *7*, 1–25.

[19] D'Addona, A.; Maffulli, N.; Formisano, S.; Rosa, D. Inflammation in tendinopathy. *Surgeon* **2017**, *15*, 297–302.

[20] Zhang, X. Y.; Eliasberg, C. D.; Rodeo, S. A. Mitochondrial dysfunction and potential mitochondrial protectant treatments in tendinopathy. *Ann. N Y Acad. Sci.* **2021**, *1490*, 29–41.

[21] Liu, Y. C.; Wang, H. L.; Huang, Y. Z.; Weng, Y. H.; Chen, R. S.; Tsai, W. C.; Yeh, T. H.; Lu, C. S.; Chen, Y. L.; Lin, Y. W. et al. Alda-1, an activator of ALDH2, ameliorates Achilles tendinopathy in cellular and mouse models. *Biochem. Pharmacol.* **2020**, *175*, 113919.

[22] Lee, J. M.; Hwang, J. W.; Kim, M. J.; Jung, S. Y.; Kim, K. S.; Ahn, E. H.; Min, K.; Choi, Y. S. Mitochondrial transplantation modulates inflammation and apoptosis, alleviating tendinopathy both *in vivo* and *in vitro*. *Antioxidants (Basel)* **2021**, *10*, 696.

[23] Li, K. Q.; Deng, G. M.; Deng, Y.; Chen, S. W.; Wu, H. T.; Cheng, C. Y.; Zhang, X. R.; Yu, B.; Zhang, K. R. High cholesterol inhibits tendon-related gene expressions in tendon-derived stem cells through reactive oxygen species-activated nuclear factor-κB signaling. *J. Cell. Physiol.* **2019**, *234*, 18017–18028.

[24] Kucukler, S.; Benzer, F.; Yildirim, S.; Gur, C.; Kandemir, F. M.; Bengu, A. S.; Ayna, A.; Caglayan, C.; Dortbudak, M. B. Protective effects of chrysin against oxidative stress and inflammation induced by lead acetate in rat kidneys: A biochemical and histopathological approach. *Biol. Trace Elem. Res.* **2021**, *199*, 1501–1514.

[25] Yardım, A.; Kandemir, F. M.; Çomaklı, S.; Özdemir, S.; Caglayan, C.; Kucukler, S.; Çelik, H. Protective effects of curcumin against paclitaxel-induced spinal cord and sciatic nerve injuries in rats. *Neurochem. Res.* **2021**, *46*, 379–395.

[26] Wei, H.; Wang, E. K. Nanomaterials with enzyme-like characteristics (nanozymes): Next-generation artificial enzymes. *Chem. Soc. Rev.* **2013**, *42*, 6060–6093.

[27] Szymanski, C. J.; Munusamy, P.; Mihai, C.; Xie, Y. M.; Hu, D. H.; Gilles, M. K.; Tyliszczak, T.; Thevuthasan, S.; Baer, D. R.; Orr, G. Shifts in oxidation states of cerium oxide nanoparticles detected inside intact hydrated cells and organelles. *Biomaterials* **2015**, *62*, 147–154.

[28] Kwon, H. J.; Kim, D.; Seo, K.; Kim, Y. G.; Han, S. I.; Kang, T.; Soh, M.; Hyeon, T. Ceria nanoparticle systems for selective scavenging of mitochondrial, intracellular, and extracellular reactive oxygen species in Parkinson's disease. *Angew. Chem., Int. Ed.* **2018**, *57*, 9408–9412.

[29] Bao, Q. Q.; Hu, P.; Xu, Y. Y.; Cheng, T. S.; Wei, C. Y.; Pan, L. M.; Shi, J. L. Simultaneous blood-brain barrier crossing and protection for stroke treatment based on edaravone-loaded ceria nanoparticles. *ACS Nano* **2018**, *12*, 6794–6805.

[30] Son, D.; Lee, J.; Lee, D. J.; Ghaffari, R.; Yun, S. M.; Kim, S. J.; Lee, J. E.; Cho, H. R.; Yoon, S.; Yang, S. et al. Bioresorbable electronic stent integrated with therapeutic nanoparticles for endovascular diseases. *ACS Nano* **2015**, *9*, 5937–5946.

[31] Kim, J.; Hong, G.; Mazaleuskaya, L.; Hsu, J. C.; Rosario-Berrios, D. N.; Grosser, T.; Cho-Park, P. F.; Cormode, D. P. Ultrasmall antioxidant cerium oxide nanoparticles for regulation of acute inflammation. *ACS Appl. Mater. Interfaces* **2021**, *13*, 60852–60864.

[32] Adebayo, O. A.; Akinloye, O.; Adaramoye, O. A. Cerium oxide nanoparticles attenuate oxidative stress and inflammation in the liver of diethylnitrosamine-treated mice. *Biol. Trace Elem. Res.* **2020**, *193*, 214–225.

[33] Soh, M.; Kang, D. W.; Jeong, H. G.; Kim, D.; Kim, D. Y.; Yang, W.; Song, C.; Baik, S.; Choi, I. Y.; Ki, S. K. et al. Ceria-zirconia nanoparticles as an enhanced multi-antioxidant for sepsis treatment. *Angew. Chem., Int. Ed.* **2017**, *56*, 11399–11403.

[34] Wang, P.; Geng, J.; Gao, J. H.; Zhao, H.; Li, J. H.; Shi, Y. R.; Yang, B. Y.; Xiao, C.; Linghu, Y. Y.; Sun, X. F. et al. Macrophage achieves self-protection against oxidative stress-induced ageing through the Mst-Nrf2 axis. *Nat. Commun.* **2019**, *10*, 755.

[35] Tohidnezhad, M.; Varoga, D.; Wruck, C. J.; Brandenburg, L. O.; Seekamp, A.; Shakibaei, M.; Sönmez, T. T.; Pufe, T.; Lippross, S. Platelet-released growth factors can accelerate tenocyte proliferation and activate the anti-oxidant response element. *Histochem. Cell Biol.* **2011**, *135*, 453–460.

[36] Gañán-Gómez, I.; Wei, Y.; Yang, H.; Boyano-Adánez, M. C.; García-Manero, G. Oncogenic functions of the transcription factor Nrf2. *Free Radic. Biol. Med.* **2013**, *65*, 750–764.

[37] Carvajal, S.; Perramón, M.; Casals, G.; Oró, D.; Ribera, J.; Morales-Ruiz, M.; Casals, E.; Casado, P.; Melgar-Lesmes, P.; Fernández-Varo, G. et al. Cerium oxide nanoparticles protect against oxidant injury and interfere with oxidative mediated kinase signaling in human-derived hepatocytes. *Int. J. Mol. Sci.* **2019**, *20*, 5959.

[38] Saita, M.; Kaneko, J.; Sato, T.; Takahashi, S. S.; Wada-Takahashi, S.; Kawamata, R.; Sakurai, T.; Lee, M. C. I.; Hamada, N.; Kimoto, K. et al. Novel antioxidative nanotherapeutics in a rat periodontitis model: Reactive oxygen species scavenging by redox injectable gel suppresses alveolar bone resorption. *Biomaterials* **2016**, *76*, 292–301.

[39] Liu, A. L.; Wang, Q.; Zhao, Z. N.; Wu, R.; Wang, M. C.; Li, J. W.; Sun, K. Y.; Sun, Z. Y.; Lv, Z. Y.; Xu, J. et al. Nitric oxide nanomotor driving exosomes-loaded microneedles for achilles tendinopathy healing. *ACS Nano* **2021**, *15*, 13339–13350.